A micromagnetic theory of skyrmion lifetime in ultrathin ferromagnetic films

Anne Bernand-Mantel[a], Cyrill B. Muratov[b,c,1,2], and Valeriy V. Slastikov[d,1]

We use the continuum micromagnetic framework to derive the formulas for compact skyrmion lifetime due to thermal noise in ultrathin ferromagnetic films with relatively weak interfacial Dzyaloshinskii–Moriya interaction. In the absence of a saddle point connecting the skyrmion solution to the ferromagnetic state, we interpret the skyrmion collapse event as "capture by an absorber" at microscale. This yields an explicit Arrhenius collapse rate with both the barrier height and the prefactor as functions of all the material parameters, as well as the dynamical paths to collapse.

magnetic skyrmions | stochastic dynamics | rare events | topological protection

Magnetic skyrmions are a characteristic example of topological solitons existing at the nanoscale. Their extensive studies in the past 10 years revealed a very rich underlying physics as well as potential applications in the field of spintronics (1–4). While the fundamental object for applications is an individual skyrmion in a homogeneous ferromagnetic environment, for topological reasons it cannot be created or annihilated by a continuous transformation from the ferromagnetic state. This transition is, however, enabled by the discrete nature of the condensed matter as observed experimentally (5–8).

The detailed physical mechanisms of skyrmion annihilation have been investigated at the nanoscale using atomic spin simulations combined with methods of finding the minimum energy path and harmonic transition state theory (9–16). In particular, the energy barrier ΔE separating the skyrmion state from the ferromagnetic state was obtained numerically for some given sets of parameters and the skyrmion annihilation rate was estimated by a simple Arrhenius law $\Gamma_0 e^{-\Delta E/(k_B T)}$, where Γ_0 is the rate prefactor, also called the attempt frequency. While early works used standard values of Γ_0 that are in the range from 10^9 to 10^{12} Hz in the macrospin model (17), more recent studies show that in the case of skyrmions Γ_0 can vary by many orders of magnitude (8, 18–20).

Despite this progress, there are limitations to the atomistic simulations. First, they are computationally expensive, which limits the accessible skyrmion sizes (usually below 5 nm in diameter) and the physical parameter ranges that can be explored. Second, the obtained results depend on the microscopic details that are not necessarily known or controlled in the case of nanocrystalline systems. Under these circumstances, there is clearly a need for a more coarse-grained theory that would provide universal relations between the skyrmion lifetime and the material parameters. Moreover, it is reasonable to expect that under many physically relevant conditions the microscopic details do not play a dominant role for fluctuation-driven skyrmion collapse. For example, the skyrmion size is often much larger than the atomic lattice spacing when it loses its topological protection via the disappearance of its core (14, 21).

In this paper, we develop a theory of skyrmion lifetime based on the continuum field theory and derive the expressions for both the energy barrier and the attempt frequency as functions of all the material parameters. Starting with the stochastic Landau–Lifshitz–Gilbert partial differential equation, we first derive several integral identities associated with the fundamental continuous symmetry groups of the exchange energy. Then, in the exchange-dominated regime, we carry out a finite-dimensional reduction of the stochastic skyrmion dynamics and obtain a system of stochastic ordinary differential equations for the skyrmion radius and angle. Finally, in the small thermal noise regime we use the obtained equations to calculate the Arrhenius rate, including the prefactor, by interpreting the skyrmion collapse event as "capture by an absorber" for the skyrmion radius at the atomic scale.

Model

At the continuum level the magnetization dynamics in an ultrathin ferromagnetic film at finite temperature are described by the stochastic Landau–Lifshitz–Gilbert (sLLG)

Significance

Skyrmions are topologically protected particle-like metastable states arising in field theories of different branches of physics, from particle physics to condensed matter. Our work brings about an advance in understanding thermal stability of magnetic skyrmions by exploiting the fundamental properties of the exchange energy and interpreting skyrmion collapse events as capture by an absorber at microscale. This yields the skyrmion collapse rate as a function of all material parameters. The methodology developed by us has a wide applicability to other physical systems in which topological defects disappear through singularity formation at the continuum level.

Author affiliations: [a]Laboratoire de Physique et Chimie des Nano-Objets, Université de Toulouse, UMR 5215 Institut National des Sciences Appliquées, CNRS, Université Paul Sabatier, F-31077 Toulouse Cedex 4, France; [b]Department of Mathematical Sciences, New Jersey Institute of Technology, Newark, NJ 07102; [c]Dipartimento di Matematica, Università di Pisa, 56127 Pisa, Italy; and [d]School of Mathematics, University of Bristol, Bristol BS8 1TW, United Kingdom

equation (17, 22–24) (for the technical details on all the formulas in this paper, see *SI Appendix*)

$$\frac{\partial \mathbf{m}}{\partial t} = -\mathbf{m} \times \mathbf{h}_{\text{eff}} + \alpha \mathbf{m} \times \frac{\partial \mathbf{m}}{\partial t}, \quad \textbf{[1]}$$

where $\mathbf{m} = \mathbf{m}(\mathbf{r}, t)$ is the unit magnetization vector at position $\mathbf{r} \in \mathbb{R}^2$ measured in the units of the exchange length $\ell_{ex} = \sqrt{2A/(\mu_0 M_s^2)}$, where A is the exchange stiffness, M_s is the saturation magnetization, and μ_0 is vacuum permeability, and time t is measured in the units of $\tau_0 = (\gamma \mu_0 M_s)^{-1}$, where γ is the gyromagnetic ratio, and α is the dimensionless Gilbert damping parameter. With the dimensionless parameters characterizing the anisotropy, the Dzyaloshinskii–Moriya interaction (DMI), and the noise strengths, respectively,

$$Q = \frac{2K}{\mu_0 M_s^2}, \qquad \kappa = D\sqrt{\frac{2}{\mu_0 M_s^2 A}}, \qquad \varepsilon = \frac{k_B T}{2Ad}, \quad \textbf{[2]}$$

where K is the magnetocrystalline uniaxial anisotropy constant, D is the DMI constant, and $k_B T$ is temperature in the energy units, the effective field $\mathbf{h}_{\text{eff}} = \mathbf{h}_{\text{eff}}(\mathbf{r}, t) \in \mathbb{R}^3$ in Eq. **1** is given by

$$\mathbf{h}_{\text{eff}} = -\frac{\delta E(\mathbf{m})}{\delta \mathbf{m}} + \sqrt{2\alpha\varepsilon}\,\boldsymbol{\xi}, \quad \textbf{[3]}$$

where $E(\mathbf{m})$ is the micromagnetic energy measured in the units of $2Ad$, with d being the film thickness, and $\boldsymbol{\xi} = \boldsymbol{\xi}(\mathbf{r}, t) \in \mathbb{R}^3$ is a suitable regularization of a three-dimensional delta-correlated spatiotemporal white noise (25). In the local approximation for the stray field and in the absence of the applied field we have (26–31)

$$E(\mathbf{m}) = \frac{1}{2} \int_{\mathbb{R}^2} \left\{ |\nabla \mathbf{m}|^2 + (Q-1)|\mathbf{m}_\perp|^2 - 2\kappa \mathbf{m}_\perp \cdot \nabla m_\parallel \right\} d^2 r, \quad \textbf{[4]}$$

which consists of, in order of appearance, the exchange, the effective uniaxial out-of-plane anisotropy ($Q > 1$), and the interfacial DMI terms, respectively. Above we defined $\mathbf{m}_\perp \in \mathbb{R}^2$ and $m_\parallel \in \mathbb{R}$ to be the respective in-plane and out-of-plane components of the magnetization vector $\mathbf{m} = (\mathbf{m}_\perp, m_\parallel)$.

Integral Identities

We begin by rewriting the sLLG equation in the spherical coordinates, setting $\mathbf{m} = (\sin\theta\cos\phi, \sin\theta\sin\phi, \cos\theta)$, and express it in terms of θ and ϕ. After some tedious algebra, we get

$$\begin{pmatrix} \alpha & -1 \\ 1 & \alpha \end{pmatrix} \begin{pmatrix} \theta_t \\ \sin\theta\phi_t \end{pmatrix} = \begin{pmatrix} \Delta\theta - \sin\theta\cos\theta|\nabla\phi|^2 \\ \sin\theta\Delta\phi + 2\cos\theta\nabla\theta\cdot\nabla\phi \end{pmatrix}$$
$$+ \begin{pmatrix} -(Q-1)\cos\theta\sin\theta + \kappa\,\sin^2\theta\nabla\phi\cdot\mathbf{p} + \sqrt{2\alpha\varepsilon}\,\eta \\ -\kappa\sin\theta\nabla\theta\cdot\mathbf{p} + \sqrt{2\alpha\varepsilon}\,\zeta \end{pmatrix}, \quad \textbf{[5]}$$

where η and ζ are two independent, delta-correlated spatiotemporal white noises, $\mathbf{p} = (-\sin\phi, \cos\phi)$, and here and everywhere below the letter subscripts denote partial derivatives in the respective variables.

We next derive several integral identities for the solutions of Eq. **5** that will be useful in obtaining the evolution equations for the skyrmion characteristics. These identities are closely related to the continuous symmetry groups associated with the exchange energy term, which dominates in the considered regime. We start

with the group of rotations and scalar multiply Eq. **5** by $(0, \sin\theta)$. A subsequent integration over space yields

$$\int_{\mathbb{R}^2} \sin\theta\theta_t \, d^2r + \alpha \int_{\mathbb{R}^2} \sin^2\theta\phi_t \, d^2r + \kappa \int_{\mathbb{R}^2} \sin^2\theta\nabla\theta\cdot\mathbf{p} \, d^2r$$
$$= \sqrt{2\alpha\varepsilon} \left(\int_{\mathbb{R}^2} \sin^2\theta \, d^2r \right)^{1/2} \dot{W}_1(t), \quad \textbf{[6]}$$

where $W_1(t)$ is a Wiener process, and the dot denotes the time derivative. Here we noted that an integral of a divergence term vanishes for the profiles that approach a constant vector at infinity.

Now we use the group of dilations and scalar multiply Eq. **5** by $(\nabla\theta \cdot (\mathbf{r} - \mathbf{r}_0(t)), \sin\theta\nabla\phi \cdot (\mathbf{r} - \mathbf{r}_0(t)))$, where $\mathbf{r}_0(t)$ is arbitrary. This yields

$$-\int_{\mathbb{R}^2} (\mathbf{r} - \mathbf{r}_0(t)) \cdot \nabla\theta \sin\theta\phi_t \, d^2r + \alpha \int_{\mathbb{R}^2} (\mathbf{r} - \mathbf{r}_0(t)) \cdot \nabla\theta \, \theta_t \, d^2r$$
$$+ \alpha \int_{\mathbb{R}^2} \sin^2\theta\nabla\phi \cdot (\mathbf{r} - \mathbf{r}_0(t))\phi_t \, d^2r$$
$$+ \int_{\mathbb{R}^2} (\mathbf{r} - \mathbf{r}_0(t)) \cdot \nabla\phi \, \theta_t \sin\theta d^2r$$
$$= \int_{\mathbb{R}^2} (\mathbf{r} - \mathbf{r}_0(t)) \cdot \nabla\theta \left(-(Q-1)\cos\theta\sin\theta + \kappa\,\sin^2\theta\nabla\phi\cdot\mathbf{p} \right) d^2r$$
$$+ \int_{\mathbb{R}^2} \sin\theta\nabla\phi \cdot (\mathbf{r} - \mathbf{r}_0(t))(-\kappa\sin\theta\nabla\theta\cdot\mathbf{p}) \, d^2r$$
$$+ \sqrt{\int_{\mathbb{R}^2} |(\mathbf{r} - \mathbf{r}_0(t)) \cdot \nabla\theta|^2 d^2r + \int_{\mathbb{R}^2} \sin^2\theta|(\mathbf{r} - \mathbf{r}_0(t)) \cdot \nabla\phi|^2 d^2r}$$
$$\times \sqrt{2\alpha\varepsilon}\,\dot{W}_2(t), \quad \textbf{[7]}$$

where $W_2(t)$ is another Wiener process. Finally, we use the translational symmetries of the exchange energy and scalar multiply the stochastic LLG equation by $(\theta_x, \sin\theta\phi_x)$ or $(\theta_y, \sin\theta\phi_y)$ to obtain two similar identities involving two other Wiener processes $W_3(t)$ and $W_4(t)$ (*SI Appendix*). Note that in general the Wiener processes $W_1(t)$ through $W_4(t)$ are not independent.

Reduction to a Finite-Dimensional System

To proceed further, we focus on the regime in which a good approximation to the solutions of the sLLG equation may be obtained by means of a matched asymptotic expansion. This regime, in which $0 < \kappa \ll \sqrt{Q-1}$, gives rise to a skyrmion profile $(\theta, \phi) = (\bar{\theta}, \bar{\phi})$ whose radius ρ_0 is asymptotically (30–32)

$$\rho_0 \simeq \frac{\kappa}{2(Q-1)\ln\left(a\kappa^{-1}\sqrt{Q-1}\right)}, \quad \textbf{[8]}$$

for some $a \sim 1$. It is characterized by a compact core on the scale of ρ_0,

$$\bar{\theta}(r) \simeq 2\arctan(r/\rho_0), \quad \textbf{[9]}$$

which is the Belavin–Polyakov profile (33) that minimizes the exchange energy at leading order, and an exponentially decaying tail on the scale of the Bloch wall length $L = (Q-1)^{-1/2}$:

$$\bar{\theta}(r) \simeq \pi - 2\rho_0\sqrt{Q-1}\,K_1(r\sqrt{Q-1}), \quad \textbf{[10]}$$

where $K_1(z)$ is the modified Bessel function of the second kind that minimizes the exchange plus anisotropy energy to the leading order. In both the core and the tail $\bar{\phi} = \psi - \pi$, where $x = r\cos\psi$

and $y = r \sin \psi$ are the polar coordinates relative to the skyrmion center.

Dynamically, one would expect that for $\alpha \sim 1$ the above profile would stabilize on the diffusive timescale $\tau_{\text{core}} \sim \rho^2$ in the core and on the relaxation timescale $\tau_{\text{relax}} \sim (Q-1)^{-1}$ in the tail, respectively. Therefore, on the timescale $\tau_{\text{relax}} \gtrsim \tau_{\text{core}}$ the dynamical profile $\theta(\mathbf{r}, t)$ in the skyrmion core would be expected to be dominated by the exchange and, therefore, stay close to a suitably translated, rotated, and dilated Belavin–Polyakov profile:

$$\theta(\mathbf{r}, t) \simeq 2 \arctan(|\mathbf{r} - \mathbf{r}_0(t)|/\rho(t)), \quad [11]$$

$$\phi(\mathbf{r}, t) \simeq \arg(\mathbf{r} - \mathbf{r}_0(t)) - \pi + \varphi(t). \quad [12]$$

Similarly, on the timescale $\gtrsim \tau_{\text{relax}}$ the skyrmion profile in the tail should approach

$$\theta(\mathbf{r}, t) \simeq \pi - 2\rho(t)\sqrt{Q-1}\, K_1(|\mathbf{r} - \mathbf{r}_0(t)|\sqrt{Q-1}). \quad [13]$$

Here, the functions $\rho(t)$, $\varphi(t)$, and $\mathbf{r}_0(t)$ may be interpreted, respectively, as the instantaneous radius, rotation angle, and center of the skyrmion.

The above approximate solution may be substituted into our integral identities to obtain a closed set of equations for $\rho(t)$, $\varphi(t)$, and $\mathbf{r}_0(t) = (x_0(t), y_0(t))$:

$$\frac{d}{dt}\begin{pmatrix} \ln \rho \\ \varphi \end{pmatrix} = -\frac{1}{1+\alpha^2}\begin{pmatrix} \alpha & -1 \\ 1 & \alpha \end{pmatrix}\begin{pmatrix} Q - 1 - \frac{\kappa \cos \varphi}{2\rho \ln(L/\rho)} \\ \frac{\kappa \sin \varphi}{2\rho \ln(L/\rho)} \end{pmatrix}$$
$$+ \sqrt{\frac{\alpha \varepsilon}{4\pi(1+\alpha^2)\rho^2 \ln(L/\rho)}}\begin{pmatrix} \dot{W}_1(t) \\ \dot{W}_2(t) \end{pmatrix}, \quad [14]$$

and

$$\dot{x}_0 = \sqrt{\frac{\alpha \varepsilon}{2\pi(1+\alpha^2)}}\, \dot{W}_3, \quad \dot{y}_0 = \sqrt{\frac{\alpha \varepsilon}{2\pi(1+\alpha^2)}}\, \dot{W}_4. \quad [15]$$

Furthermore, to the leading order the Wiener processes $W_1(t)$ through $W_4(t)$ are all mutually independent. It is understood that ρ is bounded above by some $L_0 < L$. Moreover, when $\rho \sim \rho_0$, we may set the large logarithmic factor $\ln(L/\rho)$ to a constant $\Lambda = \ln(a\kappa^{-1}\sqrt{Q-1})$ to the leading order. Introducing the new variable $\bar{z} = \bar{x} + i\bar{y} = \rho e^{i\varphi}$ then results in the following stochastic differential equation:

$$d\bar{z}(t) = -\frac{\alpha + i}{1+\alpha^2}\left[(Q-1)\bar{z}(t) - \frac{\kappa}{2\Lambda}\right]dt$$
$$+ \sqrt{\frac{\alpha \varepsilon}{4\pi \Lambda(1+\alpha^2)}}\, d\bar{W}(t), \quad [16]$$

where $\bar{W}(t) = W_1(t) + iW_2(t)$ is a complex-valued Wiener process. Note that the dynamics of $\bar{z}(t)$ decouple from those of $\mathbf{r}_0(t)$, with the latter undergoing a simple diffusion with diffusivity $D_{\text{eff}} = \frac{\alpha \varepsilon}{4\pi(1+\alpha^2)}$, in agreement with ref. 34.

Calculation of the Collapse Rate

We now focus on the analysis of Eq. **16**. It describes a two-dimensional shifted Ornstein–Uhlenbeck process, whose equilibrium measure is given by the Boltzmann distribution

$$p_{\text{eq}}(\bar{z}) = 4\Lambda \varepsilon^{-1}(Q-1)e^{-\frac{H(\bar{z})}{\varepsilon}}, \quad [17]$$

where

$$H(\bar{z}) = 4\pi \Lambda(Q-1)|\bar{z} - \bar{z}_0|^2, \quad \bar{z}_0 = \frac{\kappa}{2\Lambda(Q-1)}, \quad [18]$$

which is peaked around $\bar{z} = \bar{z}_0$ in the complex plane. This distribution is attained on the timescale of τ_{relax}.

Note that the probability of the solutions of Eq. **16** starting at $\bar{z} = \bar{z}_0$ to hit the origin is zero, although the probability to come to an arbitrarily small neighborhood of the origin is unity. Therefore, within Eq. **16** a more careful definition of the skyrmion collapse event is necessary. For that purpose, we note that when the skyrmion radius becomes sufficiently small, the continuum micromagnetic description of the magnetization profile breaks down. This happens when the skyrmion radius reaches the atomic scale, at which point the skyrmion loses its topological protection. Therefore, to model skyrmion collapse we supplement Eq. **16** with an absorbing boundary condition at $|\bar{z}| = \delta$ for some cutoff radius $\delta \ll \bar{z}_0$. In atomically thin films, this cutoff radius is on the order of the film thickness measured in the units of the exchange length, $\delta \sim d/\ell_{\text{ex}}$. The mean skyrmion lifetime may then be found by solving an appropriate boundary value problem in the plane. When $\varepsilon \ll 1$, it may be obtained by investigating the stationary solution $p = p(\bar{x}, \bar{y})$ of the Fokker–Planck equation associated with Eq. **16** with a suitable source $g(\bar{x}, \bar{y})$ away from the absorber:

$$\left[(Q-1)x - \frac{\kappa}{2\Lambda}\right](\alpha q_{\bar{x}} - q_{\bar{y}}) + y(Q-1)(\alpha q_{\bar{y}} + q_{\bar{x}})$$
$$= \frac{\alpha \varepsilon}{8\pi \Lambda}(q_{\bar{x}\bar{x}} + q_{\bar{y}\bar{y}}) + g p_{\text{eq}}^{-1}, \quad [19]$$

where we introduced $q = p/p_{\text{eq}}$ and set $q = 0$ at $|\bar{z}| = \delta$. When $\varepsilon \to 0$, we are interested in the boundary layer solution of Eq. **19** in the neighborhood of $(\bar{x}, \bar{y}) = (\delta, 0)$, in which the probability flux is concentrated (35). The function q approaches 1 away from the boundary layer. Then to the leading order in ε, the solution in a small neighborhood around the point $(\bar{x}, \bar{y}) = (\delta, 0)$ is given by

$$q(\bar{x}, \bar{y}) \simeq 1 - \exp\left\{-\frac{8\pi \Lambda}{\varepsilon}\left[(Q-1)\delta - \frac{\kappa}{2\Lambda}\right](\bar{x} - \delta)\right\}. \quad [20]$$

Assuming that $\varepsilon \ll \kappa\delta$, the corresponding total probability flux into the boundary is, to the leading order,

$$J_\delta = \frac{\alpha \varepsilon}{8\pi \Lambda(1+\alpha^2)}\int_{|\bar{z}|=\delta} p_{\text{eq}}|\nabla q|\, ds \quad [21]$$

$$\simeq \frac{\alpha \Lambda(Q-1)}{1+\alpha^2}\left[\frac{\kappa}{2\Lambda} - (Q-1)\delta\right]\left(\frac{8\delta}{\varepsilon\kappa}\right)^{1/2}e^{-\frac{H(\delta)}{\varepsilon}}, \quad [22]$$

which has the form of an Arrhenius law with explicit expressions for the barrier height $H(\delta)$ and the prefactor. Note that the latter depends weakly on the parameter $\delta \ll 1$, and to the leading order we have

$$J_\delta \simeq \frac{\alpha(Q-1)A_\delta}{1+\alpha^2}\left(\frac{2\kappa\delta}{\varepsilon}\right)^{1/2}\exp\left\{-\frac{\pi\kappa^2}{\varepsilon\Lambda(Q-1)}\right\}, \quad [23]$$

where $\pi\kappa^2/[\Lambda(Q-1)]$ is the leading-order barrier height $H(0)$ and

$$A_\delta = \exp\left\{\frac{4\pi\kappa\delta}{\varepsilon}\left[1 - \frac{\Lambda(Q-1)\delta}{\kappa}\right]\right\} > 1 \quad [24]$$

is an anomalous factor due to a small reduction $\Delta H = H(0) - H(\delta)$ of the barrier height resulting from the presence of the absorber at the microscale needed to break the topological protection.

The quantity in Eq. **23** gives the leading-order asymptotic skyrmion collapse rate for $\delta \ll 1$ as $\varepsilon \to 0$. The exponential term is nothing but the Arrhenius factor associated with the energy barrier

to collapse, to the leading order in $\kappa/\sqrt{Q-1} \ll 1$. A comparison with the result of the numerical solution for the radial skyrmion profile (*SI Appendix*) shows that taking $a = 2.8$ in the definition of $\Lambda = \ln(a\kappa^{-1}\sqrt{Q-1})$ reproduces the exact barrier height to within 17% for all $\kappa/\sqrt{Q-1} < 0.8$.

It is also possible to obtain the skyrmion collapse rate in the limit $\delta \to 0$ with $\varepsilon \ll 1$ and all the other parameters fixed, corresponding to the opposite extreme $\varepsilon \gg \kappa\delta$. Here in the $O(\varepsilon/\kappa)$ neighborhood of the absorber the function $q(\bar{x}, \bar{y})$ is, to the leading order in $\delta \ll 1$,

$$q(\bar{x}, \bar{y}) \simeq \frac{\ln\left(\frac{\sqrt{\bar{x}^2 + \bar{y}^2}}{\delta}\right)}{\ln\left(\frac{b\alpha\varepsilon}{\kappa\delta\sqrt{1+\alpha^2}}\right)}, \qquad [25]$$

where $b \approx 0.179$. An analogous computation to the one leading to Eq. **23** yields in this case

$$J_\delta \simeq \frac{\alpha(Q-1)A_\delta}{(1+\alpha^2)\ln\left(\frac{b\alpha\varepsilon}{\kappa\delta\sqrt{1+\alpha^2}}\right)} \exp\left\{-\frac{\pi\kappa^2}{\varepsilon\Lambda(Q-1)}\right\}. \qquad [26]$$

The condition $\varepsilon \gg \kappa\delta$ or, equivalently, $\delta \ll \varepsilon/\kappa$ ensures that $p_{\mathrm{eq}}(\bar{x}, \bar{y})$ does not vary appreciably across the absorber boundary, making $A_\delta \simeq 1$ as $\delta \to 0$.

Skyrmion Collapse Paths

The dynamics of skyrmion collapse in the small noise limit may be understood through the minimization of the large deviation action associated with Eq. **16** (36):

$$S = \frac{2\pi\Lambda(1+\alpha^2)}{\alpha}$$
$$\times \int_0^T \left| \dot{\bar{z}} + \frac{\alpha+i}{1+\alpha^2}\left[(Q-1)\bar{z} - \frac{\kappa}{2\Lambda}\right] \right|^2 dt. \qquad [27]$$

Minimizing over all trajectories $\bar{z}(t)$ that start at $\bar{z}(0) = \bar{z}_0$ and terminate at $\bar{z}(T) = \delta$, and then sending $T \to \infty$, one obtains the optimal collapse trajectory $\bar{z} = \bar{z}_{\mathrm{opt}}(t)$, where to the leading order in $\delta \ll 1$ we have

$$\bar{z}_{\mathrm{opt}}(t) = \bar{z}_0\left(1 - e^{\frac{\alpha-i}{1+\alpha^2}(Q-1)(t-T)}\right). \qquad [28]$$

As expected, for $\alpha \lesssim 1$ the collapse occurs on the timescale $\alpha^{-1}(Q-1)^{-1}$ and acquires an oscillatory character for $\alpha \ll 1$. The optimal path to collapse is illustrated in Fig. 1 *B, Inset*. Note

that for $\alpha \ll 1$ the skyrmion angle rotates as the skyrmion radius shrinks to zero, similarly to what is observed in current-driven skyrmion collapse (21).

Parametric Dependence of Skyrmion Lifetime

We now use the obtained formulas for the collapse rate to calculate the skyrmion lifetimes as functions of the material parameters in a typical ultrathin ferromagnetic film. For that purpose, we take the same parameters as in Sampaio et al. (5): $d = 0.4$ nm, $A = 15$ pJ/m, $M_s = 0.58$ MA/m, and $\alpha = 0.3$. This yields $\ell_{\mathrm{ex}} = 8.4$ nm, $\tau_0 = 7.8 \times 10^{-12}$ s, and $\delta = d/\ell_{\mathrm{ex}} = 0.0475$. The equilibrium skyrmion radius and lifetime τ_0/J_δ as functions of the dimensionless parameters $Q-1$ and κ are plotted in Fig. 1. The low-temperature regime corresponding to Eq. **23** is illustrated in Fig. 1*B*, while the high-temperature regime corresponding to Eq. **26** is illustrated in Fig. 1*C*. In both cases, the lifetime varies by many orders of magnitude, and this variation is dominated by the exponential dependence on the barrier height proportional to $\bar{\kappa}^2$, where $\bar{\kappa} = \kappa/\sqrt{Q-1}$ is the classical parameter that determines the transition from the ferromagnetic to the helical ground state happening at $\bar{\kappa} = 4/\pi$ (27). The lifetime increases upon increase of $\bar{\kappa}$ and is maximal when $\bar{\kappa} \sim 1$, at the borderline of applicability of our analysis.

In addition to the variation of the barrier height, we also predict a variation of the effective rate prefactor. This variation is stronger in the low-temperature case (Fig. 1*B*), where it is dominated by the anomalous factor A_δ. In this regime the rate prefactor becomes strongly dependent on the reduction in the barrier height due to the microscopic processes associated with the loss of the topological protection modeled by us by an absorbing boundary condition. This strong variation of the prefactor is similar to the strong prefactor dependence on microscopic details (layer stacking, number of magnetic monolayers, etc.) observed in recent simulations (20). In the high-temperature regime ($\varepsilon \gg \kappa\delta$), our prediction confirms that the prefactor becomes essentially independent of the microscopic details. The remaining dependence of the prefactor is dominated by its dependence on $Q-1$ due to the expected proportionality of the attempt frequency to the precession frequency $\gamma\mu_0 M_s(Q-1)$ (17).

Conclusion

To summarize, we carried out a derivation of skyrmion lifetime, using the stochastic Landau–Lifshitz–Gilbert equation within the framework of continuum micromagnetics and accounting for the loss of topological protection via an absorbing boundary
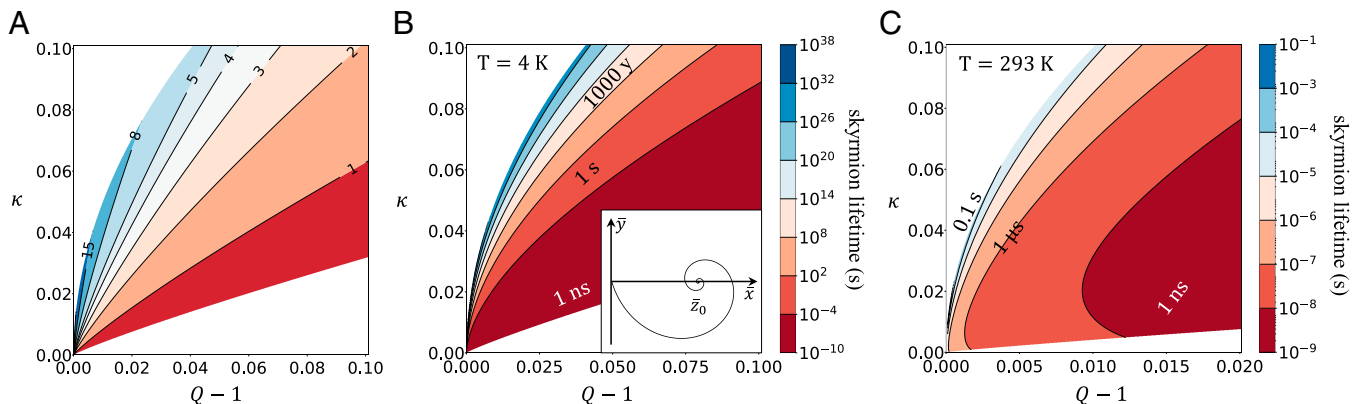
Fig. 1. (A) Skyrmion equilibrium radius $\ell_{\mathrm{ex}}\rho_0$ in nanometers, with $\ell_{\mathrm{ex}} = 8.4$ nm and ρ_0 from Eq. **8**. (B and C) Skyrmion lifetime τ_0/J_δ for $\tau_0 = 7.8 \times 10^{-12}$ s, $\alpha = 0.3$, $\delta = 0.0475$, with J_δ from Eq. **23** for $\varepsilon = 0.0046$ ($T = 4$ K) in B and J_δ from Eq. **26** for $\varepsilon = 0.337$ ($T = 293$ K) in C. In A and B, only the region $\kappa/\sqrt{Q-1} < \frac{1}{2}$ is shown. (B, Inset) The optimal collapse path $\bar{z}_{\mathrm{opt}}(t)$ from Eq. **28**.

condition at microscale. Our formulas in Eqs. **23** and **26** provide the relation of skyrmion collapse rate to material parameters and could be used as a guide in material system design in view of optimizing the skyrmion lifetime for applications. The methodology developed by us may also have a wide applicability to other physical systems in which a topological defect disappears through singularity formation at the continuum level.

Data Availability. All study data are included in this article and/or *SI Appendix*.

1. N. S. Kiselev, A. N. Bogdanov, R. Schäfer, U. K. Rössler, Chiral skyrmions in thin magnetic films: New objects for magnetic storage technologies? *J. Phys. D Appl. Phys.* **44**, 392001 (2011).
2. N. Nagaosa, Y. Tokura, Topological properties and dynamics of magnetic skyrmions. *Nat. Nanotechnol.* **8**, 899–911 (2013).
3. A. Fert, N. Reyren, V. Cros, Magnetic skyrmions: Advances in physics and potential applications. *Nat. Rev. Mater.* **2**, 17031 (2017).
4. X. Zhang et al., Skyrmion-electronics: Writing, deleting, reading and processing magnetic skyrmions toward spintronic applications. *J. Phys. Condens. Matter* **32**, 143001 (2020).
5. J. Sampaio, V. Cros, S. Rohart, A. Thiaville, A. Fert, Nucleation, stability and current-induced motion of isolated magnetic skyrmions in nanostructures. *Nat. Nanotechnol.* **8**, 839–844 (2013).
6. N. Romming et al., Writing and deleting single magnetic skyrmions. *Science* **341**, 636–639 (2013).
7. J. Hagemeister, N. Romming, K. von Bergmann, E. Y. Vedmedenko, R. Wiesendanger, Stability of single skyrmionic bits. *Nat. Commun.* **6**, 8455 (2015).
8. J. Wild et al., Entropy-limited topological protection of skyrmions. *Sci. Adv.* **3**, e1701704 (2017).
9. P. F. Bessarab, V. M. Uzdin, H. Jonsson, Method for finding mechanism and activation energy of magnetic transitions, applied to skyrmion and antivortex annihilation. *Comput. Phys. Commun.* **196**, 335–347 (2015).
10. I. S. Lobanov, H. Jonsson, V. M. Uzdin, Mechanism and activation energy of magnetic skyrmion annihilation obtained from minimum energy path calculations. *Phys. Rev. B* **94**, 174418 (2016).
11. D. Cortés-Ortuño et al., Thermal stability and topological protection of skyrmions in nanotracks. *Sci. Rep.* **7**, 4060 (2017).
12. P. F. Bessarab et al., Lifetime of racetrack skyrmions. *Sci. Rep.* **8**, 3433 (2018).
13. L. Desplat, D. Suess, J. V. Kim, R. L. Stamps, Thermal stability of metastable magnetic skyrmions: Entropic narrowing and significance of internal eigenmodes. *Phys. Rev. B* **98**, 134407 (2018).
14. B. Heil, A. Rosch, J. Masell, Universality of annihilation barriers of large magnetic skyrmions in chiral and frustrated magnets. *Phys. Rev. B* **100**, 134424 (2019).
15. I. S. Lobanov, M. N. Potkina, V. M. Uzdin, Stability and lifetimes of magnetic states of nano- and microstructures (brief review). *JETP Lett.* **113**, 801–813 (2021).
16. A. Riveros, F. Tejo, J. Escrig, K. Guslienko, O. Chubykalo-Fesenko, Field-dependent energy barriers of magnetic néel skyrmions in ultrathin circular nanodots. *Phys. Rev. Appl.* **16**, 014068 (2021).
17. W. F. Brown, Thermal fluctuations of a single-domain particle. *Phys. Rev.* **130**, 1677–1686 (1963).
18. S. von Malottki, P. F. Bessarab, S. Haldar, A. Delin, S. Heinze, Skyrmion lifetime in ultrathin films. *Phys. Rev. B* **99**, 060409(R) (2019).
19. L. Desplat, C. Vogler, J. V. Kim, R. L. Stamps, D. Suess, Path sampling for lifetimes of metastable magnetic skyrmions and direct comparison with Kramers' method. *Phys. Rev. B* **101**, 060403 (2020).
20. M. Hoffmann, G. P. Müller, S. Blügel, Atomistic perspective of long lifetimes of small skyrmions at room temperature. *Phys. Rev. Lett.* **124**, 247201 (2020).
21. A. D. Verga, Skyrmion to ferromagnetic state transition: A description of the topological change as a finite-time singularity in the skyrmion dynamics. *Phys. Rev. B Condens. Matter Mater. Phys.* **90**, 174428 (2014).
22. L. D. Landau, E. M. Lifshitz, *Course of Theoretical Physics* (Pergamon Press, London, UK, 1984), vol. 8.
23. C. J. García-Cervera, Numerical micromagnetics: A review. *Bol. Soc. Esp. Mat. Apl.* **39**, 103–135 (2007).
24. J. L. García-Palacios, F. J. Lázaro, Langevin-dynamics study of the dynamical properties of small magnetic particles. *Phys. Rev. B Condens. Matter Mater. Phys.* **58**, 14937–14958 (1998).
25. G. Da Prato, J. Zabczyk, (1992) *Stochastic Equations in Infinite Dimensions* (Encyclopedia of Mathematics and its Applications, Cambridge University Press, Cambridge, UK), vol. 44.
26. A. N. Bogdanov, D. A. Yablonskii, Thermodynamically stable "vortices" in magnetically ordered crystals. The mixed state of magnets. *Sov. Phys. JETP* **68**, 101–103 (1989).
27. A. Bogdanov, A. Hubert, Thermodynamically stable magnetic vortex states in magnetic crystals. *J. Magn. Magn. Mater.* **138**, 255–269 (1994).
28. A. Thiaville, S. Rohart, E. Jué, V. Cros, A. Fert, Dynamics of Dzyaloshinskii domain walls in ultrathin magnetic films. *Europhys. Lett.* **100**, 57002 (2012).
29. C. B. Muratov, V. V. Slastikov, Domain structure of ultrathin ferromagnetic elements in the presence of Dzyaloshinskii-Moriya interaction. *Proc. R. Soc. Lond. Ser. A* **473**, 20160666 (2017).
30. A. Bernand-Mantel, C. B. Muratov, T. M. Simon, Unraveling the role of dipolar versus Dzyaloshinskii-Moriya interactions in stabilizing compact magnetic skyrmions. *Phys. Rev. B* **101**, 045416 (2020).
31. A. Bernand-Mantel, C. B. Muratov, T. M. Simon, A quantitative description of skyrmions in ultrathin ferromagnetic films and stability of degree ± 1 harmonic maps from $\mathbb{R}^2$ to $\mathbb{S}^2$. *Arch. Ration. Mech. Anal.* **239**, 219–299 (2021).
32. S. Komineas, C. Melcher, S. Venakides, The profile of chiral skyrmions of small radius. *Nonlinearity* **33**, 3395–3408 (2020).
33. A. A. Belavin, A. M. Polyakov, Metastable states of two-dimensional isotropic ferromagnets. *JETP Lett.* **22**, 245–247 (1975).
34. C. Schütte, J. Iwasaki, A. Rosch, N. Nagaosa, Inertia, diffusion, and dynamics of a driven skyrmion. *Phys. Rev. B Condens. Matter Mater. Phys.* **90**, 174434 (2014).
35. C. W. Gardiner, *Handbook of Stochastic Methods for Physics, Chemistry, and the Natural Sciences* (Springer-Verlag, New York, NY, 1997).
36. M. I. Freidlin, A. D. Wentzell, *Random Perturbations of Dynamical Systems* (Springer, New York, NY, ed. 2, 1998).